ACS OMEGA

http://pubs.acs.org/journal/acsodf

Article

Experimental Study on a Liquid–Solid Phase-Change Autogenous Proppant Fracturing Fluid System

Yixin Chen,* Yu Sang, Jianchun Guo,* Jian Yang, Weihua Chen, Ji Zeng, Botao Tang, and Tintin He

Cite This: *ACS Omega* 2023, 8, 9101−9110

Read Online

ACCESS | Metrics & More | Article Recommendations

ABSTRACT: In this paper, a liquid−solid phase-change autogenous proppant fracturing fluid system (LSPCAP) was proposed to solve the problems that was caused by "sand-carrying" in conventional fracturing technology in oil and gas fields. The characteristic of the new fluid system is that no solid particles will be injected in the whole process of fracturing construction except liquids. The fluid itself will transform into solid particles under the formation temperature to resist the closure stress in the fractures. There are two kinds of liquids that make up the new fracturing fluid system. One of the liquids is called phase-change liquid (PCL) which occurs in the liquid−solid phase change under the formation temperature to form solid particles. Another is called nonphase-change liquid (NPCL) which controls the dispersity and size of PCL in the two-phase fluid system. Based on the molecular interaction theory and organic chemistry, bisphenol-A epoxy resin was selected as the building unit of the PCL, and the NPCL consisted of deionized water + nonionic surfactant. The test results indicated that the new fracturing fluid shows the properties of non-Newtonian fluid and has no wall-building property. The new fluid system has good compatibility with the formation fluid, conventional fracturing fluid, and hydrochloric acid. Through the filtration test, the filtration coefficients of PCL, NPCL, and mixture are found to be 1.56×10^{-4} m/s$^{1/2}$, 2.66×10^{-4} m/s$^{1/2}$, and 1.7×10^{-4} m/s$^{1/2}$, respectively, and the damage rate of mixture and NPCL is 18 and 17.7%. The friction test results show that the resistance reduction rate reaches 69% when the volume ratio of PCL and NPCL is 1:10. The shear rate and time only affect the size of the autogenous solid particles, and the sorting coefficient (S) of the particles is 1.04−1.73, indicating good sorting. Crushing resistance and conductivity test results show that the crush rate of autogenous solid particles is 3.56−8.42%. The conductivity of the autogenous solid particles is better than those of quartz sand and ceramsite under a pressure of 10−30 MPa.

1. INTRODUCTION

Hydraulic fracturing, as the main technology of oil and gas reservoir stimulation, has been widely used in oil and gas fields. Materials and techniques have advanced significantly in the decades ever since the technology was introduced in 1947. However, the conventional fracturing technology based on "sand-carrying" still has some challenges:[1]

Because of density, the solid proppant tends to settle at the bottom of the fracture quickly, which causes the accumulation of proppants at the entrance of the fractures in the process of proppant transportation.[1] In order to transport the proppants farther in fractures, raising the viscosity of the carrying fluid by adding thickening agents is widely used.[2] Although it can slow down the settlement of proppants and avoid massive accumulation of proppants at the entrance of the fractures, other problems arise.[2] For example, polymer gels may be left over as residual in the formation and cause damage.[3] Other methods such as slick water with low viscosity and large displacement can also transport the proppants farther in the fractures, but there might exist some potential risks in the construction process, with the pump pressure and friction in the pipe very high due to large displacement.[3] In addition, improper operation during fracturing construction may also cause sand plugging.[4]

In complex fracture networks, a solid proppant may not be able to turn effectively at the junction of cross fractures, which limits the distance the proppant can travel in branching fractures,[5] It may even be possible to bridge at fracture intersections, resulting in the proppant supporting only the main fracture surface.[6] However, the fracture network may be closed due to proppant-free proppant support, which reduces the conductivity of the fracture network.[7,8]

Received: August 8, 2022
Accepted: January 24, 2023
Published: March 1, 2023

https://doi.org/10.1021/acsomega.2c04853
ACS Omega 2023, 8, 9101−9110

The proppant placement formed by traditional fracturing technology is homogeneous and continuous in the form of sand bank in fractures. This placement and shape of the proppants make the oil and gas seep through the intergranular pores of solid particles, which causes limitation of reservoir stimulation.[9]

In order to solve the above problems, the liquid−solid phase-change autogenous proppant fracturing fluid system (LSPCAP) has been proposed in the paper. There are no solid particles in the whole injection process except two kinds of fluids [phase-change liquid (PCL) and nonphase-change liquid (NPCL)]. They both act as fracturing fluids and supporting solids.[2] The new fracturing fluid system can bring the following benefits:

Because of no solid injection, this fracturing is not limited by the completions of the well (such as screen section completion).[1] High viscosity of the fracturing fluid or slick water with a large placement is no longer required, which indicates that the gel residue damage, high pump pressure, and high friction in tubes can be solved. In addition, the problems such as pipeline abrasion, sand plug, and so on can also be solved.[3]

The liquids can effectively turn corners at the junction of the intersecting fractures in the complex fracture network, which causes unlimited migration of the "proppants" (liquid phase) in branch fractures. Both main planar fractures and branch fractures can be propped.[1]

Because the two kinds of liquids flow separately in fractures, the proppant placement is controlled by two-phase flow patterns without the sand bank shape, which greatly increases the fracture conductivity.[3]

2. METHODOLOGY

The LSPCAP consists of two kinds of liquids. The PCL flows in the pipe and wellbore at low temperatures and quickly transforms into solid under the formation temperature to resist closure pressure in the fracture. The NPCL stays liquid throughout the fracturing and forms an immiscible two-phase flow with the PCL. After PCL converted into solid to support fractures, the NPCL flows back and leaves the channel for oil and gas. The design principle of PCL and NPCL is as follows (Table 1).

In the above design principles, the thermal stimulation response materials can meet a series of requirements of PCL. Such materials are usually liquid prepolymers with a small molecular weight. Under heating conditions, the prepolymers change from liquid to solid by chemical reaction with the initiator, forming a linear or three-dimensional network structure.[10−15] The building units of PCL were selected by comparing the stimuli-responsive materials (Table 2).

Table 1. Design Principle of PCL and NPCL

liquids	characteristics	remarks
PCL	sensitive stimuli-responsive	recognize external stimuli; only make an established response to a single stimulus
	long-term stability	liquid long-term stability and solid long-term stability
	phase change and the cured products are controlled	the time and temperature of phase change can be controlled; the strength and hardness of the solidified product can be controlled
	chemical inertness	not react with formation fluid
	easy to inject	have low viscosity and friction resistance
	immiscible	no dissolution of PCL in NPCL
NPCL	immiscible	no dissolution of NPCL in PCL
	easy to inject	have low viscosity and friction resistance
	chemical inertness	not react with formation fluid
	the capacity to control the characteristics of PCL	the shape, size, and sorting of PCL droplets can be controlled

By comparing the advantages and disadvantages of the materials, it shows that the epoxy resin can meet the requirements of the design principle of PCL.[16−25] Therefore, bisphenol-A epoxy resin is selected as the basis of the phase-change fracturing fluid system.

According to the design principle, the basic fluid of NPCL is deionized water, its good fluidity meets the requirements of easy injection, and it is difficult to mix with organic substances (PCL). Based on the molecular interaction theory of the two-phase interface layer, PCL can be dispersed in NPCL as droplets by changing the interfacial tension between the two phases.[26−29]

(1) Reduce interface energy

Under the same volume conditions, the spherical surface area is the smallest, and the dispersed phase reduces the interface area based on the principle of minimizing the interfacial potential energy, so that the dispersed phase tends to be spherical. Thus, by adding surfactants to NPCL, the formation of dispersion systems can be achieved and the shape and size of dispersed phase droplets can be controlled.

(2) Interfacial film stability

In the dispersion system, the huge interface area and interface energy between the dispersed phase and the dispersed medium will make the droplets spontaneously coalesce to reduce the interface area and the potential energy. Therefore, the PCL/NPCL system is in a thermodynamic unstable state, and there is a dynamic process of dispersion and coalescence.

Polymers and solid particles can stabilize the interfacial membrane. Polymers can be adsorbed at the two-phase interface by diffusion and migration. Due to their links, each chain can be adsorbed on the interface to form an adsorption layer, which will make the boundary film thicker and increase the stability of the interface film. Solid particles, which are much smaller than PCL droplets and can be wetted by two-phase liquids, can be adsorbed on the interfacial layer to thicken the interfacial film and improve the interfacial strength.

3. RESULTS AND DISCUSSION

3.1. Rheological Property Test of LSPCAP. PCL and NPCL were synthesized by the above methods (see Figure 1) and evaluated experimentally. Figure 2a indicates the viscosity curve of PCL and NPCL and their mixtures with temperature. The test results show that the viscosity of PCL decreases with the increase of temperature. The viscosity of PCL decreases from 80 to 33 mPa·s when the temperature reaches 60 °C. The viscosity of NPCL is low, and the viscosity changes little with the increase of temperature. From the test results, it can be seen that the viscosity of NPCL decreases from 4 to 3 mPa s. The viscosity of the mixture varies greatly at 30−35 °C with the decrease of 40 percent (from 55 to 33 mPa·s), and it changes smoothly after 35 °C.

The test indicates that the NPCL is more prone to filtration loss due to the low viscosity. Therefore, fluid loss during fracturing needs to be improved by increasing the viscosity of nonphase-change fluids or wall building with precursors.

The viscoelastic test results are shown in Figure 2b. The test results show that with the increase of frequency, the two moduli of the mixture increase significantly, but the increase of the two

https://doi.org/10.1021/acsomega.2c04853
ACS Omega 2023, 8, 9101−9110

Table 2. Comparison of Different Stimuli-Responsive Materials as PCL's Building Units

type	advantage	disadvantage
unsaturated polyester	low phase-change temperature; simple synthesis process; good properties of the cured product	large volume shrinkage of cured product; low strength and hardness of the cured product; poor heat resistance of the cured product; poor organic solvent resistance of the cured product; phase-change accompanied byproducts produced
phenolic resin	high-temperature resistance of the cured product; good chemical stability of the cured product; simple synthesis process	low mechanical properties of cured products; low curing reaction rate; phase-change accompanied byproducts produced; high temperature required to convert solid
urea-formaldehyde resins	fast of the curing reaction rate; good chemical stability of the cured product	low mechanical properties of cured products; large volume shrinkage of the cured product; phase-change accompanied byproducts produced
epoxy resin	low volume shrinkage of the cured product; good long-term storage stability; no byproducts produced; good heat resistance of the cured product; good chemical stability of the cured product; simple synthesis process	

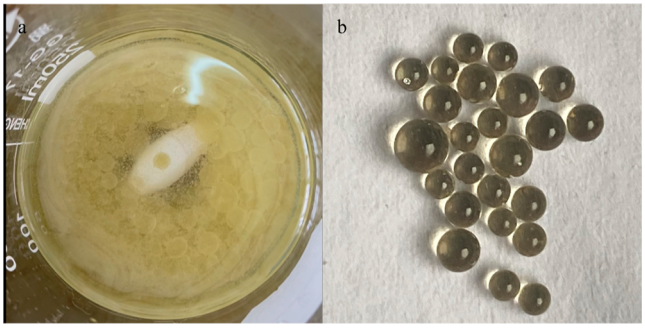

Figure 1. PCL, NPCL, and solid particles. (a) Mixture of PCL and NPCL. (b) Solid particles converting from liquid.

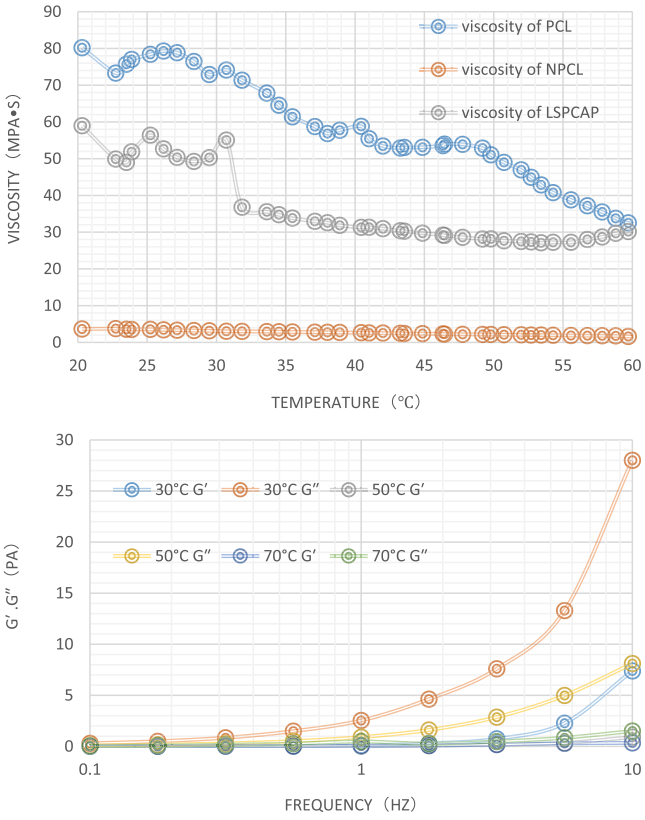

Figure 2. Temperature-viscosity curve of LSPCAP. (b) Curves of viscoelastic test at different temperatures.

moduli decreases significantly with the increase of temperature, indicating that the fracturing fluid system has obvious phase-change behavior with the increase of temperature. Comparing the storage modulus and loss modulus at the same temperature, the loss modulus is always greater than the storage modulus and the storage modulus is very small, which indicates that the strength of its deformation resistant structure is small, while the strength of its viscous internal friction structure is large. Therefore, viscosity should be taken as an important indicator for the evaluation of the new fracturing fluid system.

3.2. Compatibility Test. Figure 3 reflects the PCL mixed with five kinds of liquids commonly used during the fracturing process (volume ratio of PCL and the liquids is 1:1, and the test temperature is 20 °C). It is obvious that the interface of the mixed two-phase liquid is clear, and miscibility will not occur. Then, the test samples were heated in a water bath to 80 °C, and the PCL solidified to form a solid, which indicates that the

https://doi.org/10.1021/acsomega.2c04853
ACS Omega 2023, 8, 9101−9110

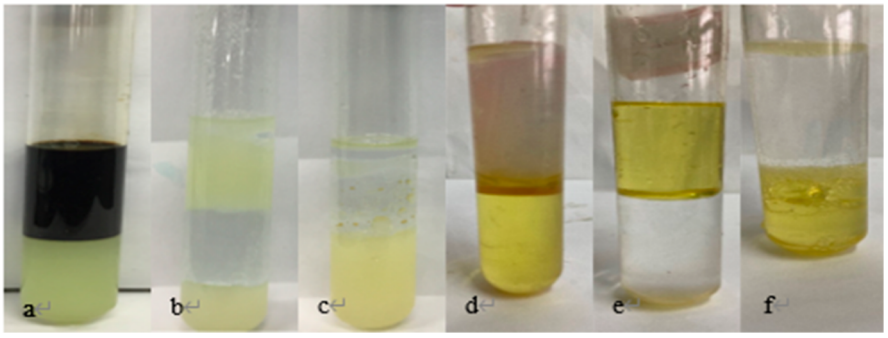

Figure 3. PCL mixed with crude oil, formation water, conventional fracturing fluid, and acid at 20 °C. (a) PCL mixed with crude oil. (b) PCL mixed with high-salinity formation water. (c) PCL mixed with low-salinity formation water. (d) PCL mixed with conventional fracturing fluid. (e) PCL mixed with hydrochloric acid. (f) Blank group.

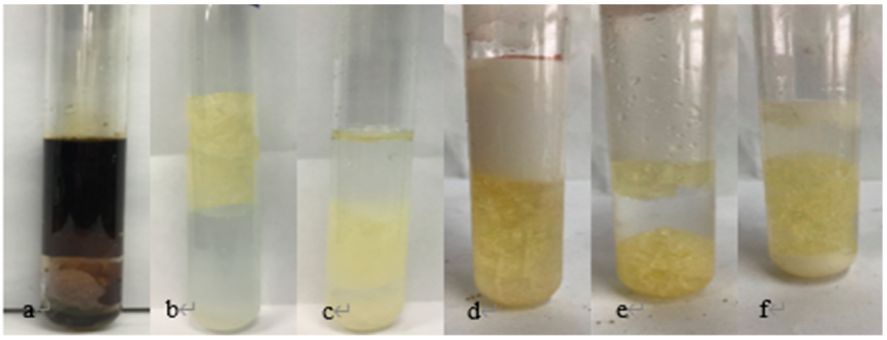

Figure 4. PCL mixed with crude oil, formation water, conventional fracturing fluid, and acid at 80 °C. (a) PCL mixed with crude oil. (b) PCL mixed with high-salinity formation water. (c) PCL mixed with low-salinity formation water. (d) PCL mixed with conventional fracturing fluid. (e) PCL mixed with hydrochloric acid. (f) Blank group.

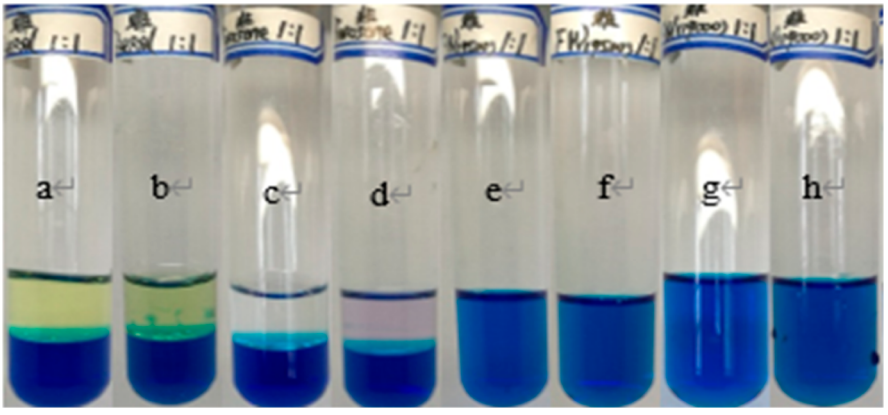

Figure 5. NPCL mixed with oil and formation water in different temperatures. (a,b) NPCL mixed with diesel oil at 25 and 80°C. (c,d) NPCL mixed with kerosene at 25 and 80°C. (e,f) NPCL mixed with high-salinity formation water at 25 and 80°C. (g,h) NPCL mixed with high-salinity formation water at 25 and 80°C.

formation water or fluids used in fracturing will not affect the phase-change behavior (see Figure 4). Figure 5 shows the NPCL mixed with five kinds of liquids commonly used during the fracturing process. It is obvious that the interface of the mixed two-phase liquid is clear, and miscibility will not occur. The test results prove that the new fracturing fluid system has good compatibility with the formation water and working fluid.

3.3. Filtration and Damage. Combined with the liquid rheology test results in Section 3.1, the LSPCAP has no wall-building property, and the fluid filtration is mainly controlled by viscosity. Through the filtration test, the filtration coefficients of PCL, NPCL, and mixture are found to be 1.56×10^{-4} m/s$^{1/2}$, 2.66×10^{-4} m/s$^{1/2}$, and 1.7×10^{-4} m/s$^{1/2}$, respectively (see Table 3), and the cumulative filtration loss of the three liquids is basically linear with time (see Figure 6a). In order to reduce the filtration of LSPCAP in the fracturing process, two main aspects are considered (improving the viscosity of NPCL or preinjection

Table 3. Filtration Test Data

<!—Col Count:5-->filtration medium	L (cm)	A (cm^2)	K (μm^2)	C_v (m/s$^{1/2}$)
PCL	2.54	5.06	0.077	1.56×10^{-4}
NPCL	2.54	5.06	0.075	2.66×10^{-4}
mixture	2.54	5.06	0.076	1.7×10^{-4}

https://doi.org/10.1021/acsomega.2c04853
ACS Omega 2023, 8, 9101−9110

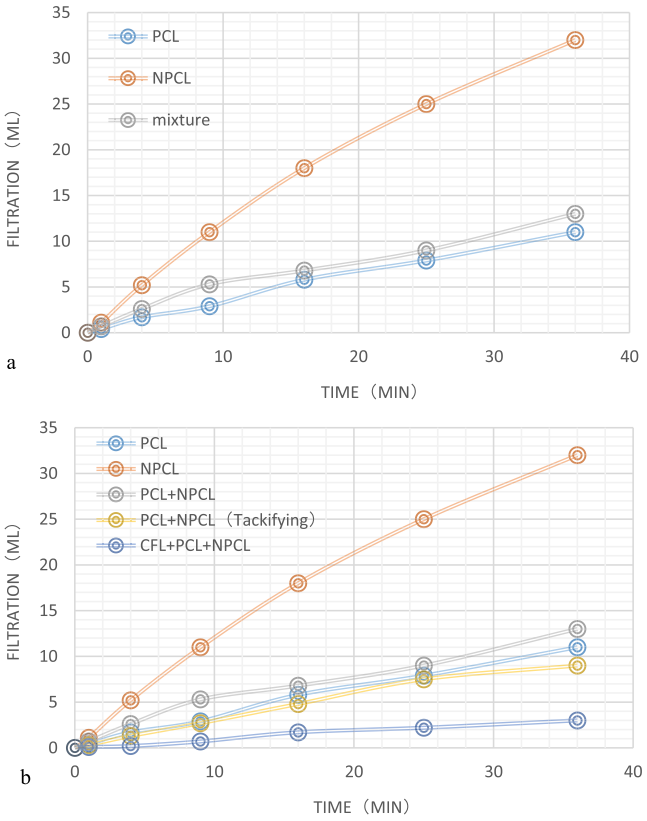

Figure 6. (a) Relationship between fluid loss and time of PCL and NPCL and their mixture. (b) Relationship between filtration and time of PCL and NPCL and their mixture and CFL.

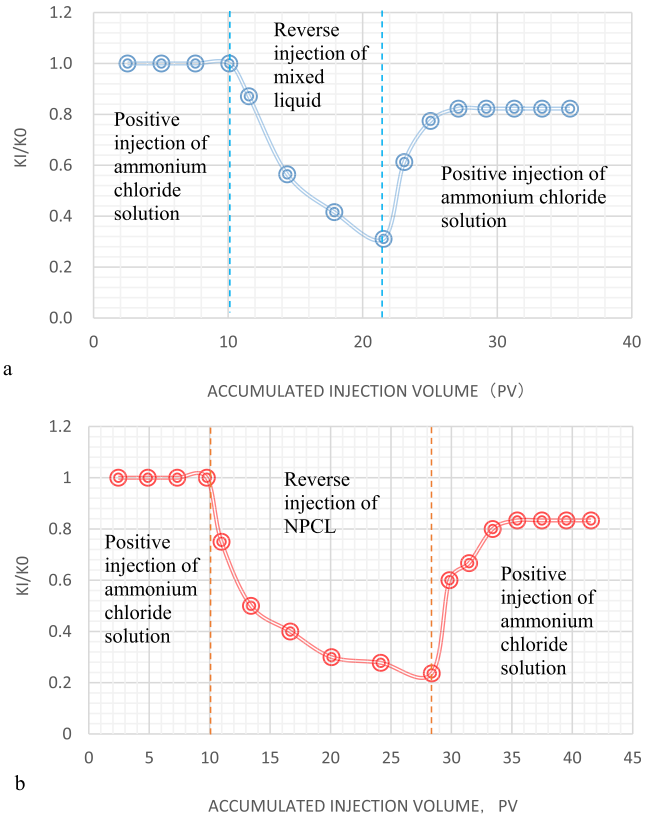

Figure 7. (a) Test results of permeability damage of the mixture of PCL and NPCL to the core matrix. (b) Test results of permeability damage of NPCL to the core matrix.

of conventional fracturing fluid for wall building). The test results are shown in Figure 6b. The filtration coefficient of the conventional fracturing fluid (CFL) + NPCL + PCL system is calculated to be 0.81×10^{-4} m/s$^{1/2}$, which decreases by 52.3% compared with the PCL + NPCL system. The filtration coefficient of the PCL + NPCL (increase viscosity) system is about 1.41×10^{-4} m/s$^{1/2}$, which decreases by 17.1% compared with the PCL + NPCL system. The test result indicates that preinjection of conventional fracturing fluid for wall building is more effective in preventing fluid loss than simply increasing the viscosity of NPCL.

Figure 7 shows the test results of permeability damage of the mixture and NPCL to the core matrix. The damage rate of the mixture and NPCL is 18 and 17.7%, respectively, which is less than 30% of the damage rate specified in SY/T 6376-2008 General Technical Conditions for Fracturing Fluids. After injection of the mixture liquid or NPCL, the permeability of the core matrix will recover to more than 80% of the original permeability in a short time, and the permeability will be stable later and will not change again. To summarize, the LSPCAP has less damage to the core matrix and can be applied in the field.

3.4. Friction Test and Optimization. The friction test results are shown in Table 4. It indicates that the pipe flow frictional resistance of the three liquids is PCL, mixture, and NPCL in the descending order; the resistance reduction rates are 20−40, 36−45, and 60−65%, respectively. With the increase of displacement, the resistance reduction rate of the three fluids all showed an increasing trend, and the resistance reduction rate of the PCL increased the most, about 20%.

To sum up, adding a friction reducer to NPCL and increasing the NPCL injection ratio can effectively reduce the pipe flow friction of liquids. Table 5 shows the relationship between the average resistance reduction rate and the PCL/NPCL volume ratio (the NPCL has been treated with friction reducer). The resistance reduction rate increases with the increase of NPCL, and it reaches 69% when the volume ratio of PCL and NPCL is 1:10.

3.5. Phase Change under Formation Conditions. Figure 8a,b shows that under laboratory conditions, the artificial cores were cut to simulate the complex fractures. Then, the cores were put into the core holder, and the temperature was increased to 80 °C. Two kinds of liquids were displaced into the core, and after 10 min, the sample was taken out to observe the phase-change results and the distribution of the autogenous proppants.

Figure 8c−e shows the autogenous proppants in the fractures. It indicated that the phase-change behavior of the new fluid system would not be affected by the complexity of the fractures, pressure, and temperature. It is obvious that the autogenous proppants filled the fractures in Figure 8c−e, which indicates that the effective diverting of liquid allowed all fractures to be filled with solid particles converted from liquid, resulting in a greatly increased, effective propped area.

Figure 8f shows the microstructure of solid particles transformed by PCL under formation conditions, demonstrating that the spherical size of particles is not affected by fracture, pressure, and temperature complexities. In short, the new fracturing fluid system has good adaptability in reservoir conditions.

3.6. Control of Shape and Size. Figure 9a−c shows the micromorphology of autogenous solid particles, quartz sand, and ceramsite. It is obvious that the autogenous solid particles have better sphericity compared with quartz sand and ceramsite,

https://doi.org/10.1021/acsomega.2c04853
ACS Omega 2023, 8, 9101−9110

Table 4. Data of Liquid Friction Test

<!—Col Count:11-->item	PCL			NPCL			mixture		
linear velocity (m/s)	10	9	8	10	9	8	10	9	8
differential pressure (Kpa)	397	366	338	226	191	163	355	311	271
water friction (Kpa)	653	531	423	653	531	423	653	531	423
resistance reduction rate (%)	39.20	31.07	20.09	65.4	64	61.5	45.64	41.43	35.93

Table 5. Average Resistance Reduction Rate of the Mixture with Different PCL/NPCL Volume Ratios

<!—Col Count:3--> PCL/NPCL volume ratio	linear velocity (m/s)	average resistance reduction rate (%)
1:10	8	69.06
1:5	8	62.53
1:3	8	53.59

which indicates that the new solid particle surface has less force per unit area and has more advantages than conventional proppants in compressive strength when bearing high loads. Figure 9d–f shows the state of autogenous solid particles, quartz sand, and ceramsite before pressure bearing, and Figure 9g–i shows the state of those after pressure bearing. It is obvious that quartz sand and ceramsite have been broken under pressure at 69 Mpa, but the autogenous solid particles have no breakage and good sphericity is also maintained. Figures 10 and 11 show that the size of the autogenous solid particles is controlled by shear rates and shear time. The particle size decreases with the increase of shear rate and shear time.

Table 6 shows the relationship between sorting of autogenous solid particles with shear time and shear rate. In the case of proppants, the better the sorting, the more uniform the force at high closure pressures, the less the proppant is to fracture or deform, and the higher the conductivity. The sorting coefficient (S) was used to characterize the quality of the autogenous solid particle sorting. When S = 1–2.5, the sorting quality was good. S = 2.5–4.5 indicates medium sorting; S > 4.5 indicates poor sorting. In the same sorting coefficient range, the smaller the value, the better the sorting. At the same shear rate, the shear time has little effect on the sorting. However, the sorting coefficient decreases with the increase of shear rate under the condition of the same shear time, which indicates the faster the shear rate, the more uniform the particle size (see Table 6).

3.7. Test and Optimization of Crushing Resistance and Conductivity. In the new fracturing fluid system, the mass fraction of RD[a] and PF[b] are greatly affected by the strength and hardness of the autogenous proppants. Therefore, the influence of different proportions of RD and PF on the mechanical properties and conductivity of the autogenous proppants was studied by combining the crushing rate experiment and the conductivity test.

The RD and PF were mixed with 16 base liquids (unmodified PCL) in different proportions (1:9, 2:8, 3:7, 4:6, 5:5, 4:1, 3:1, 2:1, and 1:1) and heated at 80 °C to form autogenous proppants. Then, the nine samples were tested using the crushing rate test and conductivity test.

Figure 12 shows the results of the crushing rate test. It is obvious to find that the proppant crushing rate decreases with the increase of RD mass fraction when the mass fraction of PF is small (PF/RD = 1:1, 1:2, 1:3, and 1:4). The crushing rate of the autogenous proppants was over 5% with a small amount of PF and RD, which could not meet the requirements of the proppant crushing resistance.

When the mass of PF exceeded 20% (PF/RD = 5:5, 6:4, 7:3, 8:2, and 9:1), the crushing rate of autogenous proppants was less than 5% and is no longer affected by the mass of RD, which indicates that the strength of autogenous proppants was controlled by the mass of PF.

Figure 8. Experimental results of phase change in complex fractures under formation conditions. (a,b) Core cutting to simulate complex fractures. (c–e) Solid particles completely fill in fractures. (f) Microstructure of solid particles cured in complex fractures.

https://doi.org/10.1021/acsomega.2c04853
ACS Omega 2023, 8, 9101–9110

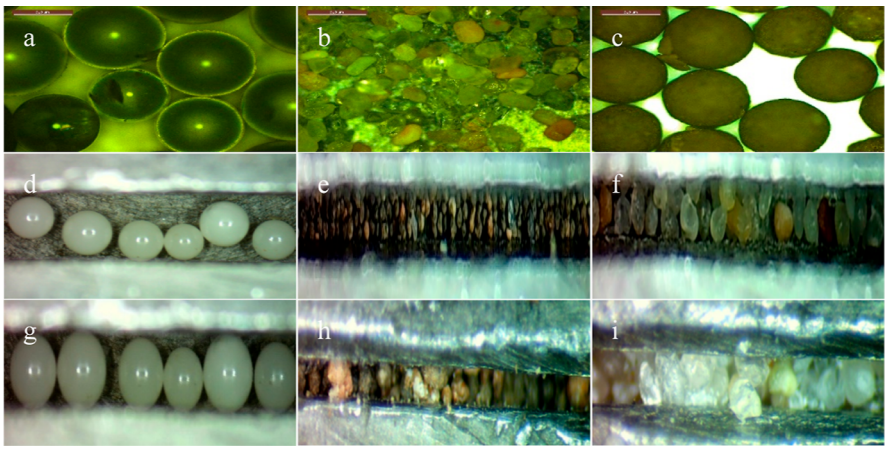

Figure 9. Sphericity comparison of solid materials before and after pressure. (a−c) Sphericity contrast of autogenous solid particles, quartz sand, and ceramsite in microstate. (d−f) Autogenous solid particles, quartz sand, and ceramsite at 0.1 Mpa. (g−i) Autogenous solid particles, quartz sand, and ceramsite at 69 Mpa.

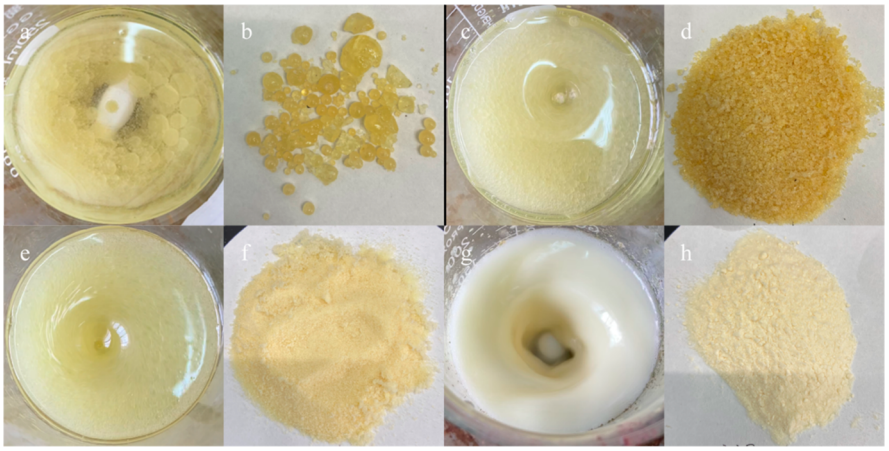

Figure 10. PCL droplet dispersion and autogenous solid particle size at different shear rates. (a,b) 80, (c,d) 160, (e,f) 240, and (g,h) 400 rpm.

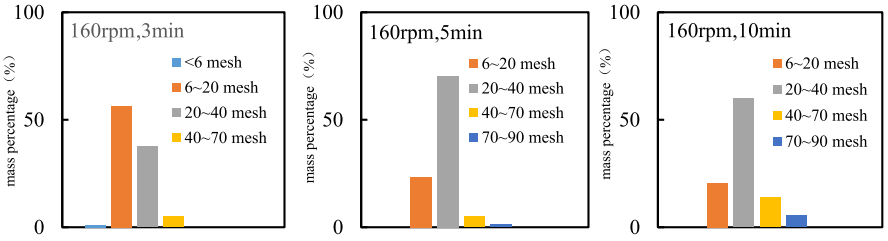

Figure 11. PCL droplet dispersion and autogenous solid particle size at different shear times.

According to the above tests, it can be considered that introducing flexible segments into the main chain or increasing the amount of the reactive diluent could significantly increase the strength and hardness of the autogenous proppants and effectively reduce the crushing rate, and PF has a more significant strength enhancement effect on the autogenic proppant than RD.

Table 7 shows the comparison of the crushing rate of the ceramic and new materials. It can be seen that the strength and hardness of the new materials with different sizes were better than those of the ceramic proppants.

Combined with the crushing rate test results, five ratios of PF and RD (9:1, 8:2, 7:3, 6:4, and 5:5) were optimized for the conductivity test. The proppant concentration was set to 5 kg/m^2, and the closure stress was set to 10−70 MPa.

Figure 13a shows the relationship of conductivity and closure stress in different ratios of PF and RD.

The test results show that the fracture conductivity of autogenous proppants is closely related to the mass of RD, which increases with the increase of RD. By measuring the deformation of the autogenous proppants before and after pressure, it was found that the sample with a low RD content would not crush under high load conditions but had a large deformation, which proves that the hardness of the autogenous proppants is controlled by RD. In other words, although the increase of PF could improve the strength and toughness of the autogenous proppants and make them difficult to crush under high load conditions, the hardness could not be fully strengthened, which caused large plastic deformation to lead to a decrease in conductivity.

https://doi.org/10.1021/acsomega.2c04853
ACS Omega 2023, 8, 9101−9110

Table 6. Sorting Coefficient of Autogenous Solid Particles under Different Shear Times and Shear Rates

shearing time (min)	shear rates (rpm)	*S*
3	80	1.71
	160	1.34
	240	1.14
	400	1.04
5	80	1.73
	160	1.17
	240	1.1
	400	1.07
10	80	1.72
	160	1.12
	240	1.13
	400	1.04

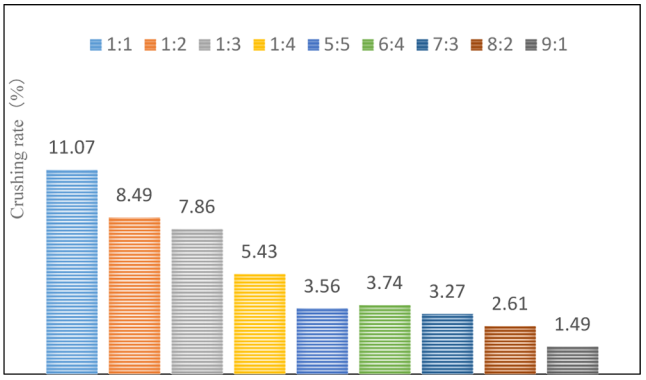

Figure 12. Experimental results of the crushing rate test.

Table 7. Comparison of the Crushing Rate between Ceramic and New Material

items	mesh	closure stress (MPa)	crushing rate (%)
the crushing rate of ceramic proppants	under 6	52	≤25
	6/20	69	≤20
	20/40	69	≤5
	40/70	86	≤10
	70/140	86	≤10
the crushing rates of new material with main sizes (RD/PF = 5:5)	under 6	52	7.66
	6/20	69	8.42
	20/40	69	3.56

The introduction of aromatic nuclei of RD improved the rigidity of the cured product. The epoxy group of RD reacted with PCL to form a three-dimensional spatial network structure during the curing reaction and made the internal structure of the molecule become closer. Macroscopically, this indicates that the cured product has higher hardness and can resist high closure stresses without deformation. Finally, the ratio of each component in the phase-change fracturing fluid is designed as RD/PF/PCL = 5:5:16.

Figure 13b shows the comparison of the conductivity of quartz sand, ceramsite, and autogenous proppants. It is obvious that the conductivity of the autogenous proppants is much higher than those of quartz and ceramsite under the condition of closure stress less than 30 MPa. The autogenous proppants' conductivity is less than that of ceramsite but always higher than that of quartz sand when the closure stress exceeds 30 MPa. The

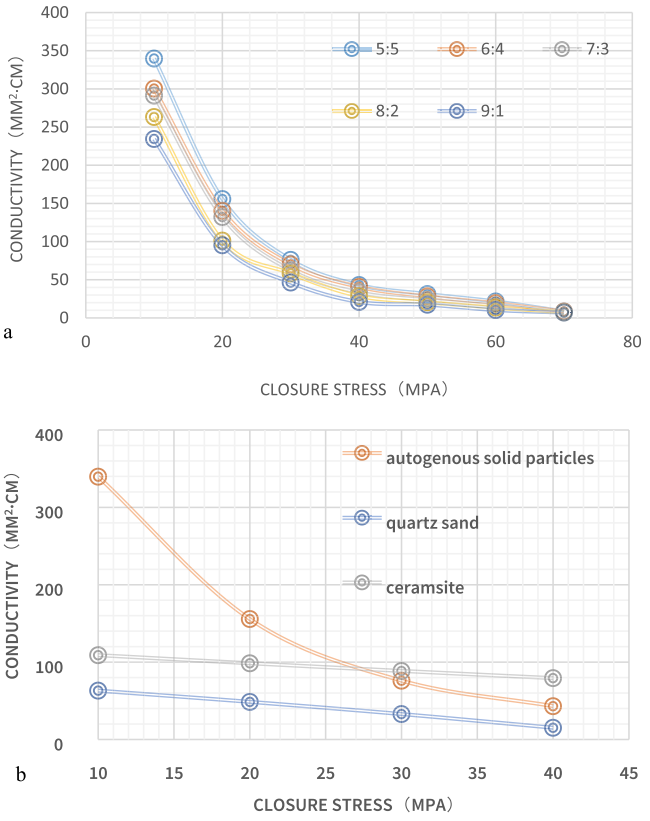

Figure 13. (a) Different conductivities of the autogenous solid particles with different ratios of RD and PF. (b) Comparison of conductivity between autogenous solid particles and conventional proppants.

test results also prove that ceramsite is more likely to be broken under high closure stress, which is consistent with the results of the breakage rate test (see Table 7). The reduced conductivity of the new material is due to deformation rather than breakage.

4. CONCLUSIONS

(1) The fracturing fluid system shows the property of pseudoplastic fluid. Its viscoelasticity is mainly characterized by the structural strength of viscous internal friction.
(2) The fracturing fluid system has good chemical inertness and good compatibility with the formation fluid.
(3) Through the filtration and damage tests, it is found that the fracturing fluid system does not have wall-building property, and the fluid filtration is mainly controlled by viscosity.
(4) The size and sorting of autogenous solid particles are mainly affected by the shear rate and shear time during the mixing process of the two-phase liquid.
(5) The conductivity of the autogenous solid particles is very high under low closure pressure, but it decays rapidly with the increase of closure pressure, which is due to the plastic deformation of the autogenous solid particles rather than breaking.

AUTHOR INFORMATION

Corresponding Authors

Yixin Chen − *PetroChina Southwest Oil and Gas Field Company, Chengdu, Sichuan 646002, China;* orcid.org/0000-0003-0234-9583; Email: 494358688@qq.com

https://doi.org/10.1021/acsomega.2c04853
ACS Omega 2023, 8, 9101−9110

Jianchun Guo − *Southwest Petroleum University, Chengdu, Sichuan 610500, China*; Email: guojianchun@vip.163.com

Authors

Yu Sang − *PetroChina Southwest Oil and Gas Field Company, Chengdu, Sichuan 646002, China*

Jian Yang − *PetroChina Southwest Oil and Gas Field Company, Chengdu, Sichuan 646002, China*

Weihua Chen − *PetroChina Southwest Oil and Gas Field Company, Chengdu, Sichuan 646002, China*

Ji Zeng − *PetroChina Southwest Oil and Gas Field Company, Chengdu, Sichuan 646002, China*

Botao Tang − *PetroChina Southwest Oil and Gas Field Company, Chengdu, Sichuan 646002, China*

Tintin He − *PetroChina Southwest Oil and Gas Field Company, Chengdu, Sichuan 646002, China*

Complete contact information is available at: https://pubs.acs.org/10.1021/acsomega.2c04853

Notes

The authors declare no competing financial interest.

■ ACKNOWLEDGMENTS

The authors would like to acknowledge the financial support of the Key projects supported by the joint fund of the National Natural Science Foundation of China (U21A20105) and the research project of proppant flowback mechanism and fiber-based proppant flowback control technique in the process of flowback after fracturing in horizontal well in Shaximiao formation tight gas reservoir of Petro-China Southwest Oil & Gas field Company (20220302-24).

■ ADDITIONAL NOTES

[a]RD is reactive diluent. Reactive diluents usually refer to low-molecular-weight compounds with one or more epoxy groups. They can directly participate in the curing reaction of the PCL and become a part of the three-dimensional network of the macromolecular structure, which can introduce functional groups into the molecular structure of the cured products in the process of the reaction.

[b]PF is compounds containing flexible fragments which can be introduced into the molecular structure of PCL to improve the toughness of the autogenous solid particles.

■ REFERENCES

(1) Chen, Y.; Sang, Y.; Guo, J.; Yang, J.; Chen, W.; Liu, F.; Zeng, J.; Tang, B. Synthesis and Characterization of a Novel Self-Generated Proppant Fracturing Fluid System. *Energies* **2022**, *15*, 8737−8758.

(2) Chen, Y. Experimental Study on a New Type of Self-Propping Fracturing Technology. Doctoral Dissertation, Southwest Petroleum University, 2017.

(3) Zhao, L.; Chen, Y.; Du, J.; Liu, P.; Li, N.; Luo, Z.; Zhang, C.; Huang, F. Experimental Study on a New Type of Self-Propping Fracturing Technology. *Energy* **2019**, *183*, 249−261.

(4) Lv, Q.; Li, Z.; Li, B.; Li, S.; Sun, Q. Study of Nanoparticle−Surfactant-Stabilized Foam as a Fracturing Fluid. *Ind. Eng. Chem. Res.* **2015**, *54*, 9468−9477.

(5) Du, D.; Li, Y.; Chao, K.; Wang, C.; Wang, D. Laboratory study of the Non-Newtonian behavior of supercritical CO2 foam flow in a straight tube. *J. Petrol. Sci. Eng.* **2018**, *164*, 390−399.

(6) Chang, F.; Berger, P.; Lee, C. In-Situ Formation of Proppant and Highly Permeable Blocks for Hydraulic Fracturing. *SPE Hydraulic Fracturing Technology Conference*; OnePetro, 2015.

(7) Tong, S.; Miller, C.; Mohanty, K. K. In situ generated proppants for shale reservoirs. *Fuel* **2022**, *319*, 123776.

(8) Yan, Z.; Dai, C.; Zhao, M.; Sun, Y.; Zhao, G. Development, formation mechanism and performance evaluation of a reusable viscoelastic surfactant fracturing fluid. *J. Ind. Eng. Chem.* **2016**, *37*, 115−122.

(9) Zhao, G.; Yan, Z.; Qian, F.; Sun, H.; Lu, X.; Fan, H. Molecular Simulation Study on the Rheological Properties of a pH-Responsive Clean Fracturing Fluid System. *Fuel* **2019**, *253*, 677−684.

(10) Zhang, W.; Mao, J.; Yang, X.; Zhang, H.; Zhao, J.; Tian, J.; Lin, C.; Mao, J. Development of a Sulfonic Gemini Zwitterionic Viscoelastic Surfactant with High Salt Tolerance for Seawater-Based Clean Fracturing Fluid. *Chem. Eng. Sci.* **2019**, *207*, 688−701.

(11) Zhang, X.; Lu, Y.; Tang, J.; Zhou, Z.; Liao, Y. Experimental Study on Fracture Initiation and Propagation in Shale Using Supercritical Carbon Dioxide Fracturing. *Fuel* **2017**, *190*, 370−378.

(12) Zhao, Z.; Li, X.; He, J.; Mao, T.; Zheng, B.; Li, G. A laboratory Investigation of Fracture Propagation Induced by Supercritical Carbon Dioxide Fracturing in Continental Shale with Interbeds. *J. Pet. Sci. Eng.* **2018**, *166*, 739−746.

(13) Pan, G.; Du, Z.; Zhang, C.; Li, X.; Yang, X.; Li, H. Synthesis, characterization, and properties of novel novolac epoxy resin containing naphthalene moiety. *Polymer* **2007**, *48*, 3686−3693.

(14) Moon, H.; Ko, D.; Park, M.; Joo, M. K.; Jeong, B. Temperature-responsive Compounds as in Situ Gelling Biomedical Materials. *Chem. Soc. Rev.* **2012**, *41*, 4860−4883.

(15) Seeboth, A.; Klukowska, A.; Ruhmann, R.; Lotzsch, D. Thermochromic Polymer Materials. *Chin. J. Polym. Sci.* **2007**, *25*, 123−135.

(16) Moon, H.; Ko, D.; Park, M.; Joo, M. K.; Jeong, B. Temperature-responsive Compounds as in Situ Gelling Biomedical Materials. *Chem. Soc. Rev.* **2012**, *41*, 4860−4883.

(17) Wang, Z.-h.; Fang, G.-Q.; He, J.-j.; Yang, H.-x.; Yang, S.-y. Semi-aromatic thermo-setting polyimide resins containing alicyclic units for achieving low melt viscosity and low dielectric constant. *React. Funct. Polym.* **2020**, *146*, 104411.

(18) Yakovlev, M. V.; Morozov, O. S.; Afanaseva, E. S.; Bulgakov, B. A.; Babkin, A. V.; Kepman, A. V. Tri-functional Phthalonitrile Monomer as Stiffness Increasing Additive for Easy Processable High Performance Resins. *React. Funct. Polym.* **2020**, *146*, 104409.

(19) Chen, S.; Yuan, L.; Wang, Z.; Gu, A.; Liang, G. Self-constructed Nano-domain Structure in Thermo-setting Blend Based on the Dynamic Reactions of Cyanate Ester and Epoxy Resins and Its Related Property. *Composites, Part B* **2019**, *177*, 107438.

(20) Du, G.; Peng, Y.; Pei, Y.; Zhao, L.; Wen, Z.; Hu, Z. Thermo-responsive Temporary Plugging Agent Based on Multiple Phase Transition Supramolecular Gel. *Energy Fuels* **2017**, *31*, 9283−9289.

(21) Wu, C.; Liu, Y.; Chiu, Y. Epoxy resins possessing flame retardant elements from silicon incorporated epoxy compounds cured with phosphorus or nitrogen containing curing agents. *Polymer* **2002**, *43*, 4277−4284.

(22) MANJUNATHA, C. M.; JAGANNATHAN, N.; PADMALATHA, K.; TAYLOR, A. C.; KINLOCH, A. J. The fatigue and fracture behavior of micron-rubber and nano-silica particles modified epoxy polymer. *Int. J. Nanosci.* **2012**, *11*, 1240002.

(23) Zhang, J.; Du, Z.; Huang, C.; Liu, W.; Li, Y. Synthesis and chiroptical properties of novel helical polyacetylenes containing fluorene pendant groups in the side chains. *React. Funct. Polym.* **2016**, *109*, 131.

(24) Kong, J.; Tang, Y.; Zhang, X.; Gu, Z. Synergic Effect of Acrylate Liquid Rubber and Bisphenol A on Toughness of Epoxy Resins. *Polym. Bull.* **2008**, *60*, 229−236.

(25) Lin, X.; Zhou, B.; Wang, C. *Synthesis and Properties of Silicone Modified Epoxy Resin*; Guangzhou Chemical Industry, 2019.

(26) Ma, S.; Liu, X.; Fan, L.; Jiang, Y.; Cao, L.; Tang, Z.; Zhu, J. Synthesis and Properties of a Bio-Based Epoxy Resin with High Epoxy Value and Low Viscosity. *ChemSusChem* **2014**, *7*, 555−562.

(27) Xu, Y.; Chen, L.; Rao, W.; Qi, M.; Guo, D. M.; Liao, W.; Wang, Y. Latent curing epoxy system with excellent thermal stability, flame retardance and dielectric property. *Chem. Eng. J.* **2018**, *347*, 223−232.
(28) Yang, S.; Zhang, Q.; Hu, Y.; Ding, G.; Wang, J.; Huo, S.; Zhang, B.; Cheng, J. Synthesis of s-triazine based tri-imidazole derivatives and their application as thermal latent curing agents for epoxy resin. *Mater. Lett.* **2018**, *216*, 127−130.
(29) Huang, K.; Liu, Z.; Zhang, J.; Li, S.; Li, M.; Xia, J.; Zhou, Y. A self-crosslinking thermosetting monomer with both epoxy and anhydride groups derived from tung oil fatty acids: Synthesis and properties. *Eur. Polym. J.* **2015**, *70*, 45−54.

https://doi.org/10.1021/acsomega.2c04853
ACS Omega 2023, 8, 9101−9110